Biomedical Physics & Engineering Express

PAPER

A wearable gait-analysis device for idiopathic normal-pressure hydrocephalus (INPH) monitoring

Erdem Atbas[1,*], **Patrick Gaydecki**[2] **and Michael J Callaghan**[3]

[1] The Department of Electrical and Electronics and School of Health Sciences, The University of Manchester, Manchester, M13 9PY, United Kingdom
[2] The Department of Electrical and Electronics, The University of Manchester, Manchester, M13 9PY, United Kingdom
[3] The Department of Health Professions, Manchester Metropolitan University, Manchester, M15 6BH, United Kingdom
[*] Author to whom any correspondence should be addressed.

E-mail: erdem.atbas@manchester.ac.uk, patrick.gaydecki@manchester.ac.uk **and** michael.callaghan@mmu.ac.uk

Keywords: biomedical wearable, gait analysis, inph diagnosis, mobility assessment

OPEN ACCESS

RECEIVED
9 May 2023

REVISED
27 January 2024

ACCEPTED FOR PUBLICATION
16 February 2024

PUBLISHED
14 October 2024

Abstract

Idiopathic Normal Pressure Hydrocephalus (iNPH) is a progressive neurologic disorder (fluid build-up in the brain) that affects 0.2%–5% of the UK population aged over 65. Mobility problems, dementia and urinary incontinence are symptoms of iNPH but often these are not properly evaluated, and patients receive the wrong diagnosis. Here, we describe the development and testing of firmware embedded in a wearable device in conjunction with a user-based software system that records and analyses a patient's gait. The movement patterns, expressed as quantitative data, allow clinicians to improve the non-invasive assessment of iNPH as well as monitor the management of patients undergoing treatment. The wearable sensor system comprises a miniature electronic unit that attaches to one ankle of the patient via a simple Velcro strap which was designed for this application. The unit monitors acceleration along three axes with a sample rate of 60 Hz and transmits the data via a Bluetooth communication link to a tablet or smart phone running the Android and the iOS operating systems. The software package extracts statistics based on stride length, stride height, distance walked and speed. Analysis confirmed that the system achieved an average accuracy of at least 98% for gait tests conducted over distances 9 m. This device has been developed to assist in the management and treatment of older adults diagnosed with iNPH.

1. Introduction

Idiopathic Normal Pressure Hydrocephalus (iNPH) is a potentially reversible neurodegenerative disease due to fluid build-up in the brain ventricles. The prevalence in the general population is still unclear but seems to affect 0.2%–5% of the UK population aged over 65 [1, 2]. NHS HES data show that the UK treats approximately 400 iNPH patients per annum, yet it is estimated that 40,000 patients are undiagnosed. iNPH is commonly characterised by a triad of cognitive decline, urinary incontinence and gait disturbance. iNPH currently is one of the only reversible forms of dementia so an accurate diagnosis is imperative in its management.

Advancements in diagnosis and treatment have aided in properly identifying and improving symptoms in patients [3]. However, a large proportion of iNPH patients remain either undiagnosed or misdiagnosed as Alzheimer's, Parkinson's or Creutzfeldt–Jakob disease. Studies have found that up to 80% of patients improve with surgical insertion of a ventriculoperitoneal shunt [4, 5]. However, the outcome of shunt surgery worsens with the progression of the disease, highlighting the importance of early diagnosis.

However, diagnosis usually requires invasive investigations such as brain CT scan, lumbar puncture for cerebrospinal fluid, or drainage and infusion tests [6–12]. The triad linked with iNPH usually begins with symmetrical gait dysfunction characterised by broad based, small-stepped instability and difficulty initiating movements. There are known scales to objectify iNPH gait symptoms, but these do not measure gait in real time. The objective assessment of these latter symptoms, often characterised by a shuffling or unstable gait, are addressed in this study. We report a technological

solution that enables non-invasive remote sensing of a patient's gait by means of a wearable device that tracks movement patterns. These data may be easily accessible by clinicians to improve the diagnosis of iNPH, as well as monitor the management of patients undergoing treatment to reverse the condition. Better diagnosis and management of iNPH would improve treatment and management of this condition, deliver social and economic benefits and, in addition, alleviate stresses on public health services. Although there is available a wide range of full-body gait analysis systems intended for clinical use, these are often expensive, video-based instruments that require careful calibration and expertise in deployment [13–15].

As far as the authors are aware, the system described here is not duplicated elsewhere, is cheap, simple to configure and may be used in either a clinical or domestic environment. We emphasise that the novelty of this method does not reside within the miniature wearable device—such commercial systems are widely available—but on the embedded firmware and user-software that performs the acquisition, transmission, analysis and statistical treatment of the data. As far as we are able to ascertain from a review of the literature, no comparable wearable system is currently available for this specific purpose [16]. The wearable system described here, together with its firmware and software, is not primarily intended for the diagnosis of iNPH (although it can assist with this). Rather, it is primarily a tool to assess changes in the gait of patients already diagnosed with this disease, for example, in response to the insertion of a shunt. From this perspective, it is a management aid, for both the patient and the clinician.

2. Methodology

2.1. Sensor system

There is available a wide range of wearable consumer electronic devices for the recording of physical activity. The growth in this market has been fuelled by rapid advances in microelectromechanical systems (MEMS), which allow force sensors such as accelerometers and gyroscopes to be encapsulated in miniature form. Further, low power wireless communication systems such as Bluetooth and ZigBee provide a means of conveniently transmitting information without the requirement for cables that may interfere with motion being studied. The system described here employs a commercial wearable device motion-tracking sensor, the Movella DOT [17], (formerly Xsens DOT), shown in figure 1, that is equipped with a triaxial accelerometer, gyroscope, and magnetometer. Only information from the accelerometer and gyroscope were used in this application; data from the magnetometer were redundant and therefore discarded. The integrated sensor employs a wireless communication module designed for short-range data transmission, Bluetooth Low Energy (BLE). It is compatible with various smart devices such as android phones, tablets, iPhones and iPads. When the sensor is synchronised with a smart device using BLE, it is possible to stream 3-axis acceleration to the connected smart device for further data analysis.

Figure 1. The movella DOT, shown with its holder.

2.2. Step data acquisition

Software in the form of a mobile app was developed for both Android and iOS operating systems to calculate stride length, foot height, speed and distance. The app allows data to be acquired at a sample rate of 60 samples per second for each axis, plotted and also transferred to a computer for further analysis (described in detail in section 3). Since acceleration describes the rate of change in velocity, it is possible to reconstruct the speed and the distance travelled by integrating the acceleration data once or twice respectively. To do this, it is important to accurately identify the samples between foot lifts and heel strikes and integrate over those data points. The sensor is attached to the patient's ankle (either left or right) using a Velcro strap designed for this research programme, with the logo on the wearable facing forwards, as shown in figure 2(a). In detail, the placement of the device is on the frontal plane within 10 cm of the ankle, allowing for it to be attached to either ankle. Securing the device in its position is crucial to prevent slippage along other axes. Additionally, the device should be positioned perpendicular to any of the axes, since this guarantees the accurate measurement of gravity, registering values within the range of −9.81 to +9.81. This is therefore necessary for the algorithm to calculate correctly. This orientation is convenient since the major (length) dimension of the sensor is aligned vertically with the patient's shin. Note that in this orientation, the axes with respect to the accelerometers are now rearranged, with the x-axis aligned vertically, the y-axis aligned horizontally and orthogonal to the direction of motion, and the z-axis aligned parallel to the direction of motion, as depicted in figure 2(b).

Under static conditions, i.e. when there is no movement of the ankle, the acceleration along the x-axis is a constant 9.81 ms^{-2} due to gravity and the accelerations along the other two axes are zero. From

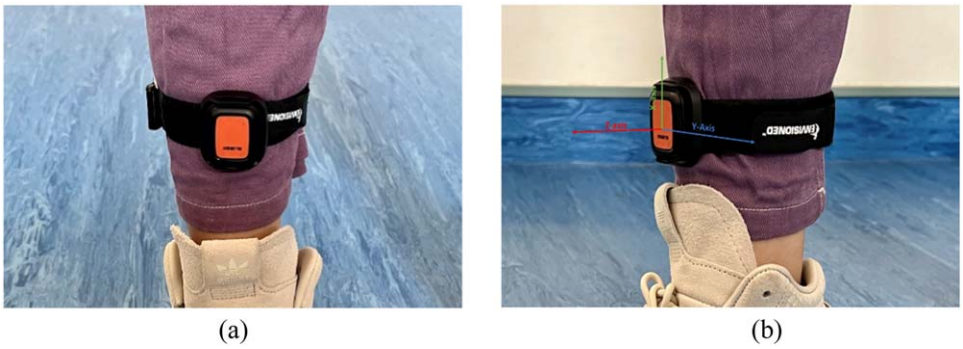

Figure 2. Showing (a) sensor attachment and (b) alignment of axes.

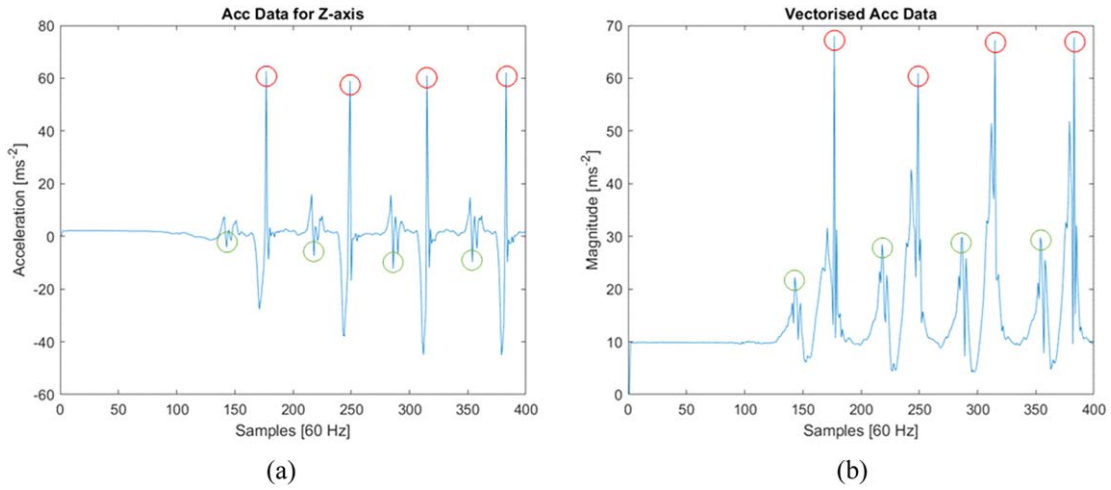

Figure 3. Showing (a) *z*-axis data and (b) vectorised data for gait fragment. Green circles denote foot lift and red circles denote heel strike.

figure 2(a), acceleration along the *y*-axis provides information on left or right sway, whereas the *z*-axis component is used to determine forward acceleration. This configuration always yields accurate quantitative measurement of walking motion. Although under movement, the gravitational force will partially affect the *z*-axis accelerometer (due to the upswing), and similarly, the forward acceleration will influence the *x*-axis accelerometer, these artefacts are minor and can be eliminated using high pass filtering. This method was used in the initial analysis; however, after further testing, it was found that if Reimann's integral method is applied it is possible to ignore the effect of gravity [18]. Figure 3(a) shows *z*-axis accelerometer data in which foot lift and heel strike are indicated; figure 3(b) shows the same activity but uses data from all three axes in vectorised form (hence the trace shows only positive values).

Since filtering is a compute intensive process, employing this technique on handheld devices is not advised. Because Reimann's integral operates on the differences between the number rather than the area under the graph, it is possible to ignore the effects of the gravity if the data are vectorised. As shown in figure 3, it is straightforward to determine by manual inspection both foot lift and heel strike; however, this process must be performed automatically by the software to ensure convenience, ease of use and repeatability.

2.3. Automation of step analysis

As given in figure 3, the foot lift and heel strike are characterised as two peaks with a short interval between them. This interval is clearly inversely proportional to the speed of walking. Automated analysis requires an adaptive algorithm that can quickly determine when the foot is lifted, and the heel struck. To achieve this, the following steps are applied:

- Vectorisation. The vector sum Acc_v for each datum point is calculated, i.e.

$$Acc_v = \sqrt[2]{Acc_x{}^2 + Acc_y{}^2 + Acc_z{}^2} \quad (1)$$

- Artefactual data generated during system initialization is stripped from the array to ensure that the readings consist only of the patients' movement

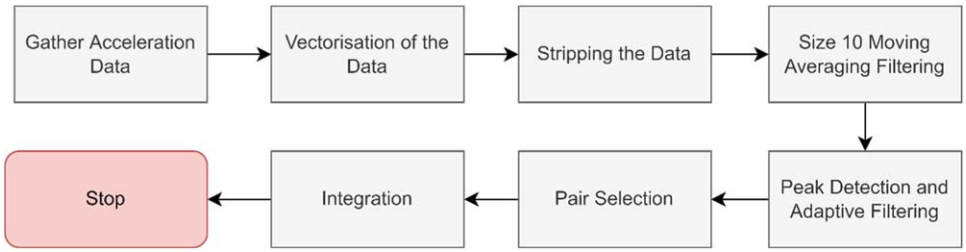

Figure 4. Flowchart of the algorithm.

patterns. During initialization, the Movella DOT populates the buffers that capture data from the accelerometers with values of zero until the device records data. Thus, captured acceleration data contains one or more zero values. Additionally, in cases where the device fails to provide a sample while sampling at a rate of 60 frames per second, a zero value is provided.

- Data are then analysed for rates of change using a 9-point moving averaging filter. The averaged data $\mathrm{Acc_{Avg}}$ is calculated as:

$$Acc_{Avg} = \frac{1}{9}\sum_{i=0}^{8} Acc_v[\mathrm{n} - i] \tag{2}$$

- The rate of change is compared between the samples. If a sudden increase is observed within this average, that sample is selected to be a candidate indicating foot lift or heel strike. Amplitudes are compared adaptively with every other sample within their region to acquire the best matched foot lift and strike pairs. The comparison process involves evaluating the instantaneous change in gravity, denoted as Acc_g, and oriented in this instance in the negative x direction. In addition, the raw magnitude of the current data is compared to that of the previous sample using an adaptive ratio to determine if it represents a local maximum. The process of selection can be broken down into the following steps.

$$Acc_{Avg}[n] > 0 \tag{3}$$

$$Acc_{Avg}[n] \geqslant \left(\frac{Acc_{Avg}[n-1]}{Acc_{Avg}[n-2]}\right) Acc_{Avg}[n-1] \tag{4}$$

$$Acc_g[n] \geqslant Acc_g[n-1] \tag{5}$$

- The selected step regions are integrated with a modified Riemann integral to convert the acceleration data, which is in $\mathrm{ms^{-2}}$ to m, cm, and $\mathrm{ms^{-1}}$. This conversion is then applied to calculate the stride length of each step, average walking speed, total travelled distance, and the foot height in each step. The Riemann integral is defined as:

$$\int_{L_f}^{S_h} Acc_{Avg}(t)\mathrm{d}t = \sum_{i=L_f}^{S_h} Acc_{Avg}[i]\,\Delta i \tag{6}$$

where L_f denotes denotes foot lifting, S_h heel strike, t detonates time, and Δi denotes the width of each sample interval, here equal to 1/60s. The entire algorithmic process is depicted in figure 4.

3. Mobile app development

To deploy any app developed for the Movella DOT, it is necessary that the host smart device supports the BLE protocol. Movella provides development frameworks for a range of operating systems, but here we focus on the apps that we have developed for both Android and iOS. The Android app was written in Java and developed using Android Studio; the iOS version was written in Objective-C using XCode. Both apps have the same functionality, so below we limit our description to the Android version. The program comprises three software modules: scan, measurement and analysis. The scan module is responsible for scanning and connecting to the sensor; the measurement module handles the acquisition and the storage of the data from the sensor to the smart device; the analysis module oversees the analysis of the acquired data.

3.1. Scan module

The scan module is the first screen that the user sees when the app is opened, figure 5(a). When the user clicks the Scan button, the program starts to scan for available Bluetooth devices and identifies the Movella Dot sensor if powered on. The user may now select the sensor to initiate a connection. To ensure seamless data gathering, the app will automatically reconnect to it in the event of a temporary loss of communication. The app also has the ability to connect to multiple sensors simultaneously; whenever a new Movella DOT device is detected, it automatically creates all the subsequent handlers, and upon its connection, all those handlers are activated automatically. (Note that the Android operating system only permits support for seven Bluetooth connections.) The scan module includes a renaming feature, allowing a particular sensor to be associated with the name of a patient or

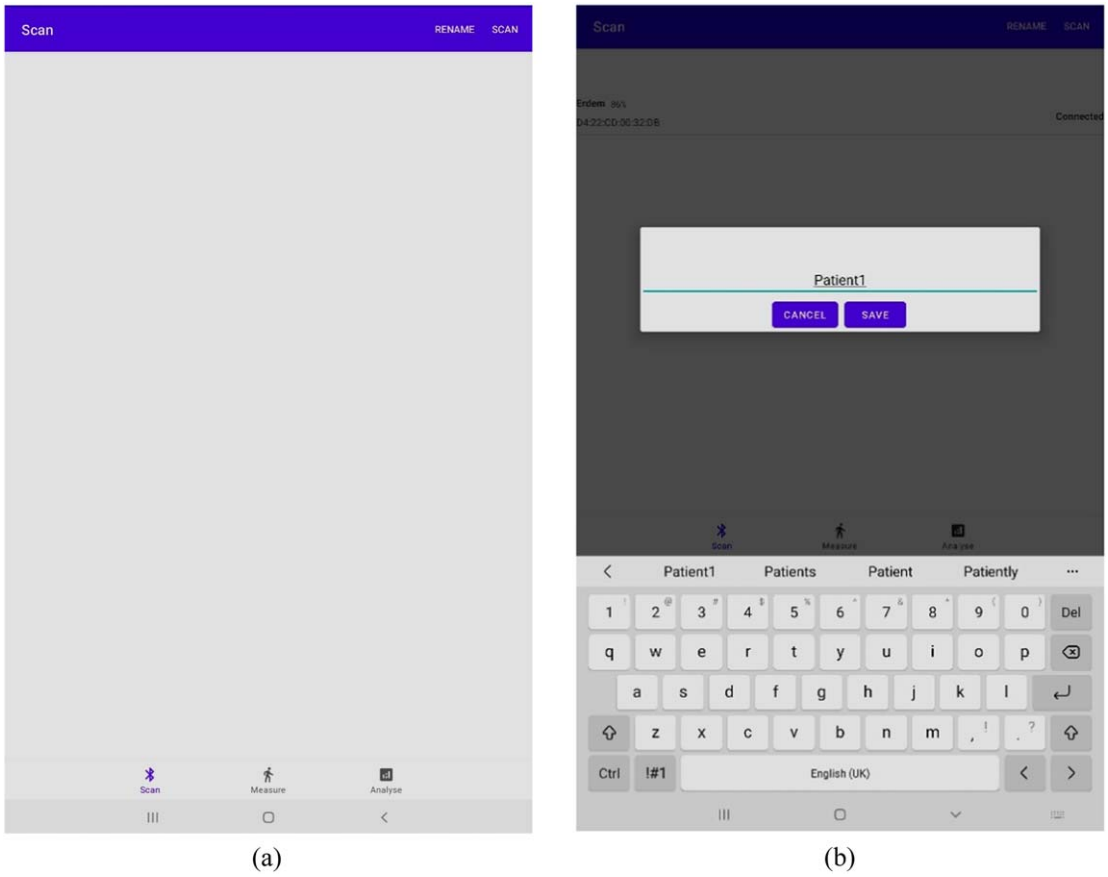

Figure 5. Showing (a) the scan module on start-up and (b) the renaming feature.

his or her unique ID. This feature is selected by tapping on the Rename button in the top right corner. The user will be prompted by a pop-up screen where in which the user enters a name or ID of up to sixteen characters, figure 5(b).

3.2. Measurement module

The measurement module, figure 6(a), handles the reception and storage of the foot motion information transmitted by the sensor. When the user clicks the Start Measuring button, the code first performs a communication integrity check with the sensor. Prior to each test initiation, the device undergoes an automatic calibration process facilitated by the connected mobile device. This calibration procedure, which typically lasts approximately 30 seconds, is an integral part of the Movella DOT's proprietary software. This calibration uses the acceleration due to gravity and is therefore independent of other sources of reference. It is imperative to note that bypassing this stage is not feasible within the device's functionality. If this check fails, the program shows a warning alert. Once the check is successful, the program synchronises with the Movella DOT. It then shows a notification that measurement will commence in five seconds, after which it performs data acquisition for 60 seconds; the Stop Measuring button allows the user to halt recording at any stage during this period. During the measurement process, two charts of live data are displayed for each sensor: orientation and acceleration respectively; further, each chart comprises three plots for the x, y and z-axes, as shown in figure 6(b). Data are saved on the smart device in CSV format, as well as to the memory of the sensor for diagnostic purposes. Once the user exits the measure module, to maintain confidentiality, the charts are destroyed. If the user decides to re-enter the measurement module, all stored data are cleared.

3.3. Analysis module

This module performs an analysis of the acquired data, generating statistics from the CSV file stored on the smart device. These statistics comprise:

- Minimum, maximum and average stride length
- Minimum, maximum and average stride height
- Average speed
- Distance walked

The analysis is selected simply by touching the Analyse button; a typical results screen is shown in figure 7.

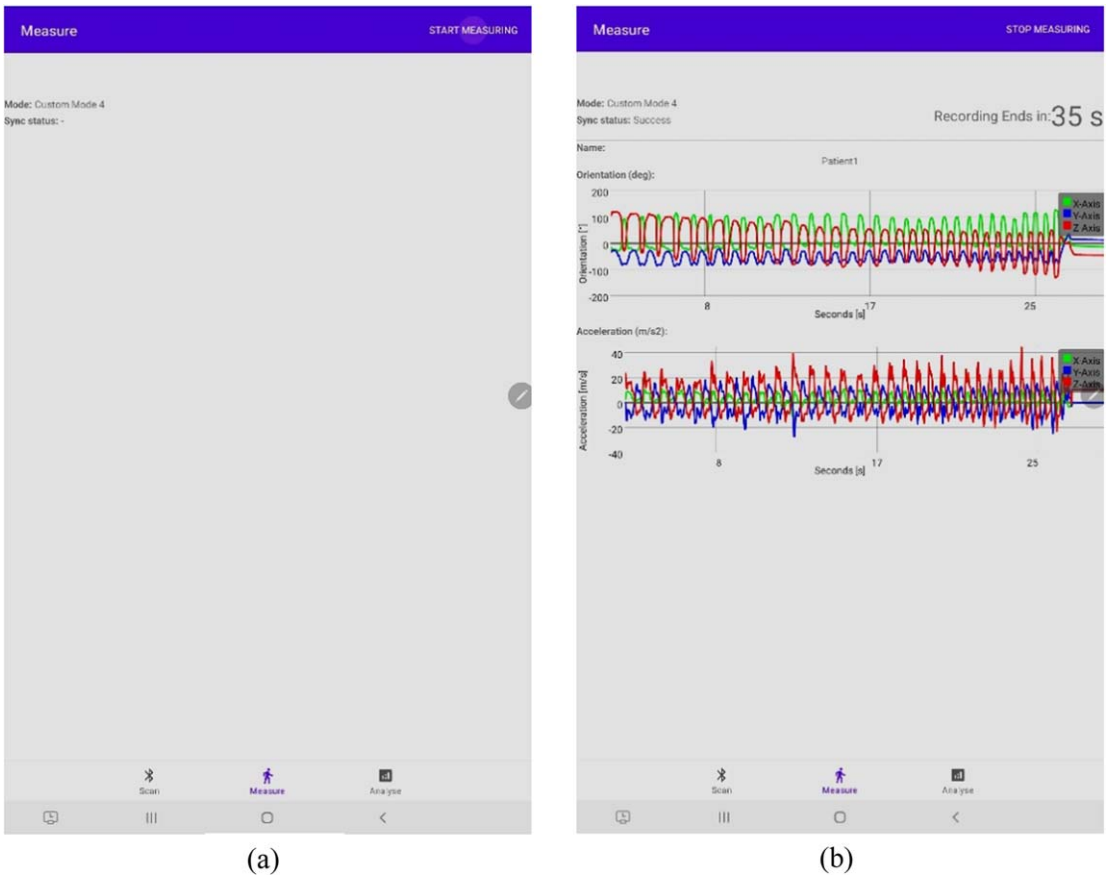

Figure 6. Showing (a) the measure module on start-up and (b) the live recording stage, which charts both orientation and acceleration for x, y and z-axes.

4. Results

4.1. Foot lift and heel strike validation

The algorithm's ability to identify the points in the data sequence corresponding to foot lift and heel strike were compared against manual visual assessment of the trace data; under repeated tests, the algorithm performed reliably and accurately. This was important, since the foot lift and heel strike measurements are used subsequently by the algorithm to calculate stride length, stride height, distance walked and speed. Tests were conducted on three healthy subjects, S1 to S3. Most of the tests were conducted using subject S1, with the smaller data sets collected from S2 and S3 used to corroborate the findings.

The foot lift and heel strike validation comprised five walking exercises, each of which included seven episodes conducted over 5 m, 12 m, 50 m, 100 m, 250 m, 500 m and 1000 m. Hence the total test distance was 9585 m. The total number of steps was 9351, yielding a mean stride length of 1.03 m. Although hundreds of comparisons were made, for the sake of brevity table 1 includes only ten examples taken from a test conducted over 12 m for volunteer V1. As indicated, there was zero error between visual assessment and the algorithm's estimation. Although this might at first appear unrealistic, the method employed by the machine algorithm was based upon a quantitative equivalent of that used for visual scrutiny; it is not surprising, therefore, that there is a perfect agreement between the two.

4.2. Walking test assessments, subject S1

To verify the accuracy of the algorithms, four walking tests were conducted by healthy volunteers from the research team and aged between 23–28 years.

The assessments:

- were conducted for the purposes of evaluation only,
- did not collect or access personally identifiable information,
- did not gather information that could be considered sensitive or personal,
- did not involve volunteers from vulnerable or dependant groups,
- did not risk disclosure of illegal or unprofessional conduct.

For these reasons, our institution's Ethics Decision Tool software determined that ethical approval was not required for these assessments.

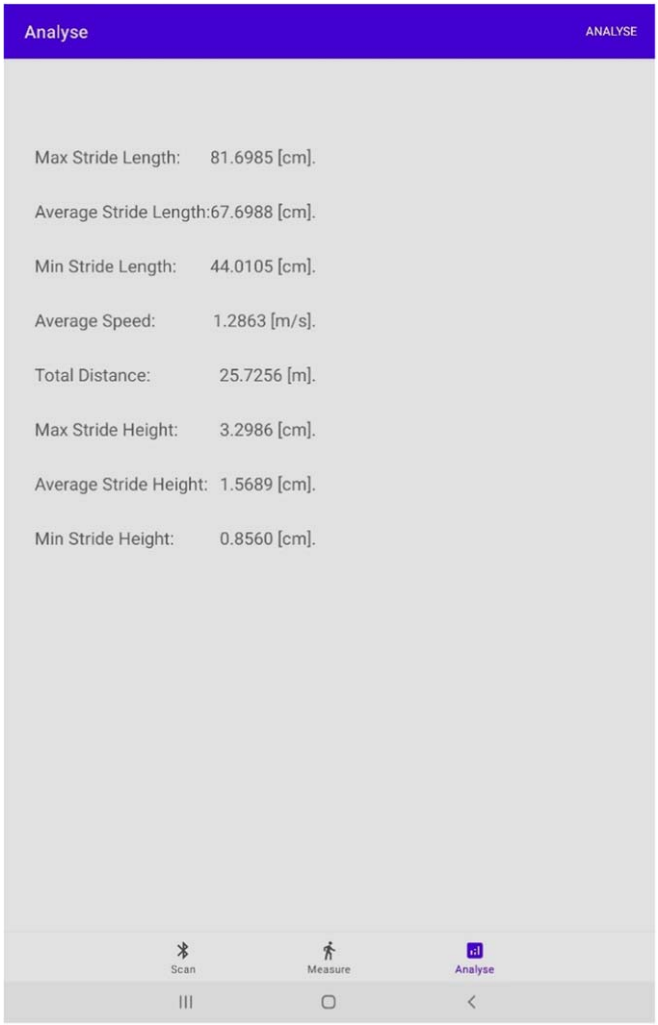

Figure 7. Results from the analysis section displayed by the app.

Table 1. Human versus automatic detection, subject S1.

	Foot lift		Heel strike	
Sample no.	Visual	Algorithm	Visual	Algorithm
1	142	142	176	176
2	217	217	248	248
3	285	285	314	314
4	353	353	382	382
5	421	421	449	449
6	488	488	512	512
7	553	553	581	581
8	618	618	647	647
9	684	684	713	713
10	754	754	778	778

The results used are summarised in table 2. Each test was conducted over two distances of 5 m and 12 m, along a corridor with a hard, smooth surface (concrete base with laminate flooring); at an average walking speed of 1.5 ms^{-1}, tests over 5 m took 3.3 s and tests over 12 m took 8 s; figure 8 shows a full posture image of a subject taken during a test, with the walkway used.

Table 2. Testing regime for stride accuracy determination, subject S1.

Test distance (m)	No. trials, starting with sensor foot	No. trials, starting without sensor foot	Total distance (m)
5	50	50	500
12	50	50	1200
	Overall distance (m)		1700

Each test was repeated 100 times; further, 50 tests started with the foot wearing the sensor and 50 without. This test protocol is summarised in table 2. The accuracies were established by comparing the stride lengths returned by the algorithm to those measured manually; using a tape measure, the distances of 5 m and 12 m were marked out, and the number of steps counted during each test. This gave a mean stride length for each test. Table 3 shows the statistics for sensor accuracy.

Tests over 5 m. If the participant commenced walking using the foot to which the sensor was attached, the accuracy of the measurements varied

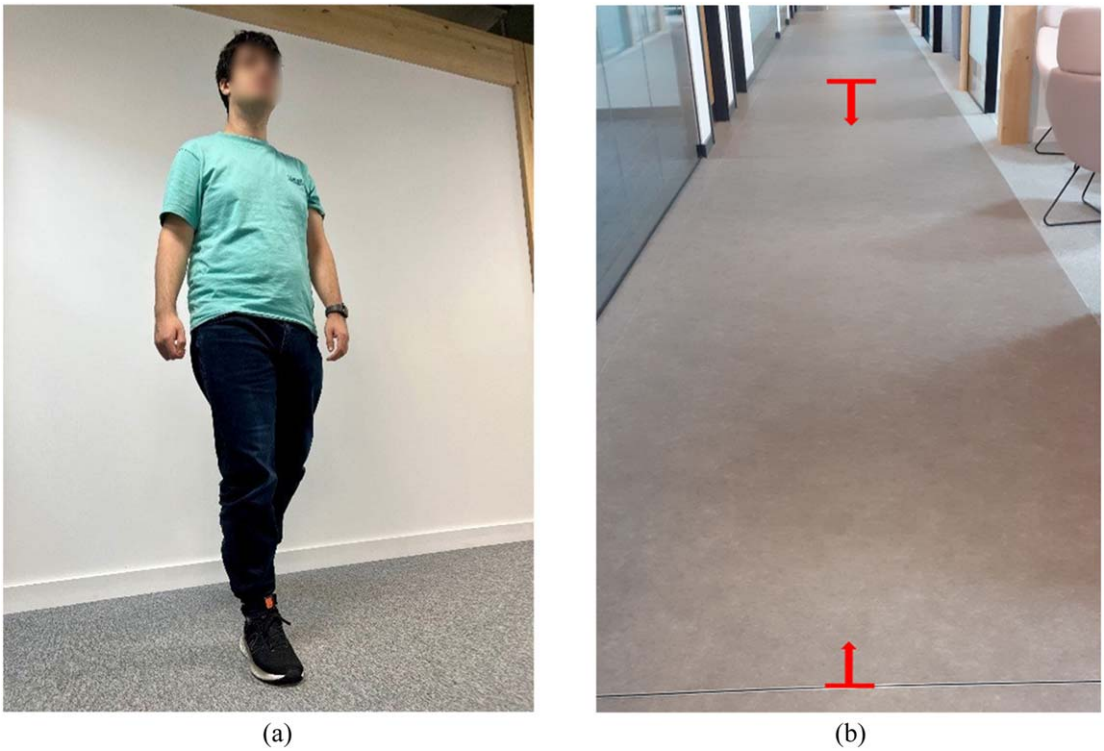

Figure 8. (a) Subject during a measurement test; (b) Walkway used in tests.

Table 3. Sensor accuracy of distance measurement, subject S1. Sensor on left foot, total of 200 trials.

Distance, m	No. trials	Starting foot	Absolute mean	Mean % Error	SD
5	50	Left	4.38	12.5	10.5
5	50	Right	4.76	4.9	6.8
12	50	Left	11.28	6.0	7.3
12	50	Right	11.52	4.0	3.5

between 62.6% to 99.8%, with an average of 87.5% and an SD of 10.5%. However, if the tests commenced with the foot not wearing the sensor, the accuracy of the measurements improved, with a range of 77.5% to 99.9%, an average of and a smaller SD of 6.8%.

Tests over 12m. If the participant commenced walking using the foot above which the sensor was attached, the accuracy of the measurements varied between 83.1% to 99.8%, with an average of 94% and an SD of 7.3%. If the tests commenced with the foot not wearing the sensor, the accuracy of the measurements once again improved, with a range of 84% to 99.5%, an average of 96% and a SD of 3.5%.

From a statistical perspective, the *a priori* assumption is that the distribution of the distance measurements conforms to the central limit theorem (CLT). Formally, the central limit theorem states that for a random sample of size n, where n is sufficiently large, the distribution of those sample means will be approximately normal (i.e. follows a Gaussian distribution), regardless of the shape of the original population distribution. The approximation becomes more accurate as the sample size increases. The CLT assumes independence of the random variables, identical distribution, and a sufficiently large sample size. Violations of these assumptions can affect the validity of the theorem. In this case, the distribution of the distance measurements is also affected by the test distance, with smaller errors associated with longer distances. This is confirmed by figures 9(a) and (b), which show the distribution of distance measurements over 50 right foot tests taken over 5 m and 12 m respectively. Figure 9(a) shows a close approximation to a normal distribution; counterintuitively, figure 9(b) displays a greater deviation from this distribution. However, this is because the errors are much smaller (note the range of distance across the x-axis) relative to the distance (12 m as opposed to 5 m) and the resolution of the histogram is constrained by the number of tests.

4.3. Walking test assessments, subject S2

A small systematic error was discovered with the above tests; there was a slight inconsistency with the starting and end locations of the toe positions with respect to the demarked lines. Walking tests were therefore

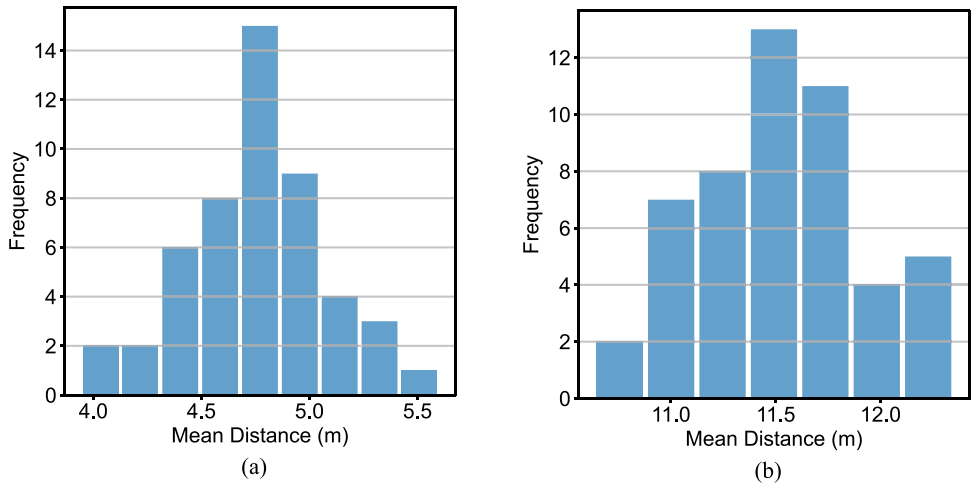

Figure 9. Distribution of distance measurements for right foot tests conducted over (a) 5 m and (b) 12 m.

Table 4. Sensor accuracy of distance measurement, subjects S2 and S3. Sensor on left foot, total of 40 trials.

Distance, m	Subject	No. trials	Starting foot	Absolute Mean	Mean % Error	SD
9	S2	10	Left	8.82	2.0	0.3
9	S2	10	Right	8.97	0.3	0.1
9	S3	10	Left	8.99	0.1	0.3
9	S3	10	Right	9.00	0.0	0.1

repeated with subjects S2 and S3, with careful attention paid to the toe positions at the start and end of each walking episode. The data are given in table 4. Each test was conducted over 9 m, with the sensor again attached above the left foot in all cases. The results confirm a higher level of accuracy, with slightly better precision returned when the first stride was taken by the foot not wearing the sensor. It is worthy of note that the walking test assessments establish the accuracy of the algorithm, not the accuracy of how the subject (or patient) covers a specific distance.

5. Discussion

This study has investigated the role of a non-invasive wearable device to assist in the assessment of patients with a diagnosis of iNPH, and in particular, to quantify the benefits conferred by the insertion of a shunt. Remote clinical monitoring and telemedicine and rehabilitation have increased in popularity [19] and have proven benefits with respect to economic costs, the patient experience and convenience for healthcare professionals and patients alike. They are still areas which need continuing research [20]. It is important to note that the diagnosis of iNPH can be challenging due to overlapping symptoms with other conditions, such as Parkinson's disease or normal aging. Therefore, an interdisciplinary approach involving neurologists, neurosurgeons, and neuropsychologists is often necessary to make an accurate diagnosis [3]. It typically involves a range of tests which may include:

1. Medical history and physical examination: The clinician will review the medical history of the patient and conduct a thorough physical examination, including a neurological assessment, and enquire about the symptoms and their progression over time.
2. Symptom evaluation: iNPH is characterized by a triad of symptoms, including gait disturbance (difficulty walking), cognitive impairment (memory and thinking problems), and urinary incontinence. The presence and severity of these symptoms will be evaluated.
3. Lumbar puncture (spinal tap): This procedure involves inserting a needle into the lower back to collect a sample of cerebrospinal fluid (CSF) for analysis. In iNPH, the CSF pressure is typically within the normal range, but drainage of a small amount of fluid may temporarily relieve symptoms, confirming the potential for improvement with treatment.
4. Brain imaging: Imaging tests are crucial in diagnosing iNPH and to exclude other conditions. Techniques commonly used include:

a. Magnetic Resonance Imaging (MRI). This is used to visualise the brain structure and identify any

abnormalities, such as enlarged ventricles (the fluid-filled spaces in the brain), which are often observed in iNPH.

b. Positron emission tomography (PET). These studies evaluate blood flow in the brain and can help determine if impaired blood flow is contributing to the symptoms.

c. Computed Tomography (CT): Such scans provide detailed images of the brain and detect any structural abnormalities or ventricular enlargement.

Despite the range of tests available, iNPH is often misdiagnosed due to lack of clinical awareness. The above tests are often conducted in specialist centres but lack of capacity within some hospital setting contributes to the low diagnoses and impacts the monitoring and treatment of patients. This wearable device acts in complement to diagnostic tools, since it tracks movement patterns, providing data that are non-invasive, readily accessible to clinicians to improve assessment of iNPH, as well as monitoring the management of patients undergoing treatment. (It may assist in diagnosis, respecting symptom evaluation, above). The device requires less than one minute to attach, and its use in combination with a smart phone allows testing to be conducted within either a clinical setting or remotely in a patient's home. In the latter setting, the data can be transferred automatically to a secure server or a cloud-based site for subsequent analysis [21].

Improvement in the assessment accuracy and the management of iNPH would reduce the cost of care for this population and improve overall patients' health, social and economic outcomes. For example, the average annual care cost for dementia in the UK is £32,250 per person. Currently 39% of dementia patients live in care homes. Using remote assessment, this device could enable 429 people to stay in their own home saving up to £14M per year, a number that will grow each year as additional patients are treated [22].

It is emphasised that thus far, the effort has focused on the engineering development, with an emphasis on accuracy of performance and ease of use. Hospital-based clinical trials are now being arranged, the results from which will be reported in a later publication.

6. Conclusion

The main purpose of this study was to assess a novel wearable device to assist in the accurate non-invasive diagnosis of iNPH. The proven capability allows the device to be studied in monitoring disease progression and to assess the efficacy of treatment. Tests confirm that the device generates quantitative information which is accurate and reliable.

Data availability statement

The data needs to be anonomised before sharing. The data that support the findings of this study are available upon reasonable request from the authors.

ORCID iDs

Erdem Atbas https://orcid.org/0000-0002-1196-8397

References

[1] Martín-Láez R *et al* 2015 Epidemiology of idiopathic normal pressure hydrocephalus: a systematic review of the literature *World Neurosurg* **84** 2002–9
[2] Andersson J *et al* 2019 Prevalence of idiopathic normal pressure hydrocephalus: a prospective, population-based study *PLoS One* **14** e0217705
[3] Nassar B R and Lippa cf 2016 Idiopathic normal pressure hydrocephalus: a review for general practitioners *Gerontology and Geriatric Medicine* **2** 2333721416643702
[4] Toma A K *et al* 2013 Systematic review of the outcome of shunt surgery in idiopathic normal-pressure hydrocephalus *Acta Neurochir (Wien)* **155** 1977–80
[5] Matsuoka T, Fujimoto K and Kawahara M 2022 Comparison of comfortable and maximum walking speed in the 10-meter walk test during the cerebrospinal fluid tap test in iNPH patients: a retrospective study *Clin Neurol Neurosurg* **212** 107049
[6] Service N H 2022 *Hydrocephalus.* [cited 2022; Available from https://nhs.uk/conditions/hydrocephalus/
[7] Wiese J and Guidry M 2012 Chapter 61. Gait Abnormalities *The Patient History: An Evidence-Based Approach to Differential Diagnosis, 2e* ed M C Henderson *et al* (The McGraw-Hill Companies)
[8] Raybaud C 2020 *Principles of Neuroimaging, in Textbook of Pediatric Neurosurgery* ed C Di Rocco *et al* (Springer International Publishing) pp 109–31
[9] Di Rocco C and Frassanito P 2020 Hydrocephalus: generalities and clinical presentations *Textbook of Pediatric Neurosurgery* ed C Di Rocco *et al* (Springer International Publishing) p. 297–332
[10] Hrishi A P and Sethuraman M 2019 Cerebrospinal Fluid (CSF) analysis and interpretation in neurocritical care for acute neurological conditions *Indian J Crit Care Med* **23** S115–s119
[11] Green J 2000 *9 - Neuropsychological Profiles IV: Traumatic Brain Injury, Substance-Related Disorders, Normal Pressure Hydrocephalus, Metabolic and Toxic Disorders, in Neuropsychological Evaluation of the Older Adult* ed J Green (Academic Press) 147–67
[12] Williams M A and Malm J 2016 Diagnosis and treatment of idiopathic normal pressure hydrocephalus *Continuum Minneap Minn* **22** 579–99
[13] Qualisys. Gait module 2023 Available from: https://qualisys.com/analysis/gait/?gclid=Cj0KCQiAx6ugBhCcARIsAGNmMbiEbsXil_Ih_naIi46moHe3nu323-8QDFdIp2OELC6_CbV_TovX-DcaArqSEALw_wcB
[14] Tekscan. F-Scan 2023 Available from: https://tekscan.com/products-solutions/systems/f-scan-system
[15] Tekscan. Strideway 2023 Available from: https://tekscan.com/products-solutions/systems/strideway-system
[16] Mualem W *et al* 2022 Utilizing data from wearable technologies in the era of telemedicine to assess patient function and outcomes in neurosurgery: systematic review and time-trend analysis of the literature *World Neurosurg* **166** 90–119

[17] Movella. Movella Dot 2023 [cited 2023; Available from https://movella.com/products/wearables/movella-dot
[18] Axler S 2020 *Riemann Integration*. 1–12
[19] LeBrun D G *et al* 2022 Telerehabilitation has similar clinical and patient-reported outcomes compared to traditional rehabilitation following total knee arthroplasty *Knee Surg Sports Traumatol Arthrosc* **30** 4098–103
[20] Seron P *et al* 2021 Effectiveness of telerehabilitation in physical therapy: a rapid overview *Phys Ther* **101**
[21] Msayib Y *et al* 2017 An intelligent remote monitoring system for total knee arthroplasty patients *J. Med. Syst.* **41** 90
[22] Society A S 2023 Available from https://alzheimers.org.uk/blog/how-much-does-dementia-care-cost